

# BUILDING ZONE MODELLING ADAPTED TO THE STUDY OF TEMPERATURE CONTROL SYSTEMS

## INTRODUCTION

The aim of this study is the development of zone models for a toolbox of dynamic models of HVAC components ([Hus97]).

Zone models exist with different levels of complexity: from simple “well mixed” models with one air node representing the whole air volume in the room to complex computational fluid dynamic (CFD) models solving the equations of conservation of mass, momentum and energy.

The simple models on the one hand are commonly used to study the energy consumption in buildings ([TRN96], [DO89]).

CFD models, on the other hand ([PHO91]), are used for comfort studies and the prediction of airflow in rooms as they provide detailed conditions in the room. Since CFD calculations are very time consuming, they are mostly used for static problems. To date, transient phenomena are rarely studied ([Rat98]).

A perfect model for control studies would unify fast simulation speed and a detailed description of the internal zone conditions. The fast simulation is useful since long term simulations are carried out. At the same time, the conditions at the temperature sensor of the controller are of particular interest.

Depending on the emitter used and the position of the sensor, there can be a temperature difference between the air at the centre and the air at the controller sensor.

To date, mostly “well mixed” models are used for control studies ([Klin99], [Rou97], [Lar80], [Hav98], [Os96], [Kast98]). In some cases, zonal models or, rarely, CFD models are used ([Peng96], [Rat98]). But these cases are limited to one specific case. However, these models are not generic and can hardly be reused for other zones or emitters.

## PHENOMENA IN A ZONE AND THEIR EFFECT ON A CONTROLLER SENSOR

A zone model adapted to the study of control systems has to provide all necessary information for the model of controller (including sensor). It is thus important to have a clear understanding of the physical quantities measured by the controller sensor in order to model all phenomena necessary for the controller.

The measurement depends on the heat exchanged by convection, conduction and radiation between the sensor and its environment (cf. figure 1, table 1). The partition of heat exchanged depends on the position of the sensor box, the type of sensor or the position of the sensor in the sensor box. An adapted zone model should thus take into account the three phenomena with a similar level of complexity.

The conductive and the radiative parts depend mainly on the modelling of the wall structure of the zone. The convective phenomena rely mainly on the modelling of the room air.

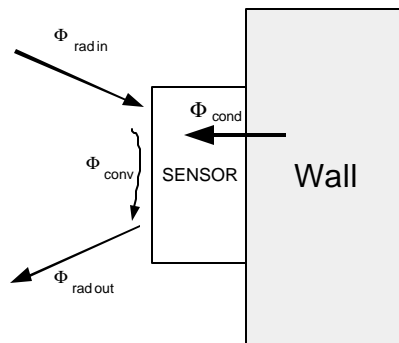


Table 1: Input variables in the sensor model

Conductive	- Wall temperature behind sensor
Radiative	- Surface temperatures in the zone
Convective	- Air temperature at sensor position - Air velocity at sensor position

Figure 1: Measurement of the sensor of a room controller

The error while modelling radiative and conductive phenomena is reduced by increasing the grid number in the modelled wall. Nevertheless the precision of the wall modelling must be comparable to

that of the internal air volume. The modelling of convective phenomena (zone air) depends on the convective coupling of the emitter and the room air. These phenomena can vary strongly from one emitter to another and even for different emitter loads. The main convective phenomena are presented in figure 2.

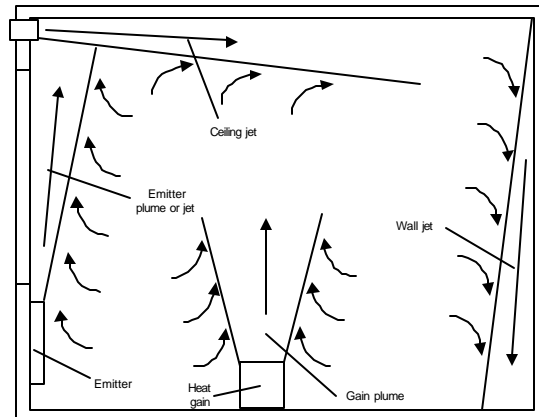


Figure 2: Main convective phenomena in a heated/ cooled room

The main phenomena can be grouped in three parts. Those are:

- Plumes (free plumes and wall plumes)
- Wall jets (ascending and descending)
- Jets (horizontal and vertical)

Plumes are created from radiators, convectors or convective heat sources in the room. They drive room air into the plume and carry this air to the ceiling. In the case of a temperature difference between the room air and the walls, a wall jet is developed. The orientation depends on the sign of the temperature difference. In general, wall jets are interesting for control studies since the sensor of the controller is often placed on a wall. If a VAV system or a fan coil is used, a jet (horizontal or vertical) appears.

### STATE OF THE ART

Different authors have integrated these phenomena in their modelling. [Peng96] developed a zone model for a fan coil application based on pre-simulations in CFD. Since the sensor was, in his case, placed at the air extraction of the fan coil unit, it was not necessary to model convective phenomena around the sensor (wall jet). The main assumption in his modelling was that the airflow in the zone does not change and is only a function of the fan speed of the fan coil. This type of model cannot be generalised.

[Rat98] developed a “quasi-transient” CFD model for a climate chamber; the model runs in real time. This technique requires remodelling of the zone for other room sizes or adaptation of the model for other applications.

In this study, simple but generic models shall be developed. The models have to include the main phenomena so that the user can simulate similar cases simply by changing the parameters of the model.

### STUDIED CASE

This paper is limited to the case of a zone equipped with a hot water radiator. The sensor can be positioned at different places in the room. It is either integrated in the valve of the radiator or placed on one of the walls beside or opposite the emitter. At the latter positions the sensor is influenced by the wall jet (see Figure 2). The difference of these air temperatures shall be analysed in the next chapter in order to show their importance on the study of controllers.

# ANALYSIS OF CENTRE AIR AND SENSOR AIR TEMPERATURE AND VALIDATION OF MODELS BY EXPERIMENTAL DATA

## EXPERIMENTAL SET UP

Test series are carried out to analyse the phenomena and to validate models. The test cell used consists of walls, ceiling and floor with embedded water circuits. The external conditions can thus be controlled by heating/cooling the panels. The interior side of the panels is covered with polystyrene for insulation (100mm) except one wall representing a window (figure 4). This “external” wall is maintained at a temperature corresponding to the inner surface temperature of the window.

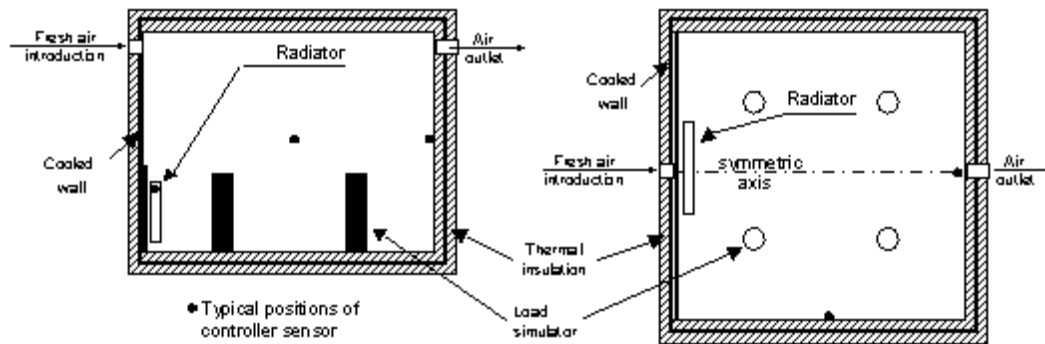


Figure 4: Test cell for the experimental validation

The room is equipped with a hot water radiator and load simulators (to represent all kind of internal gains) generating convective and radiative power. Both heat sources are installed symmetrically in the room.

Both, open loop tests and closed loop tests are carried out. The latter is finally used to validate the assembling of models (zone-emitter) through emulation (real controller).

The open loop tests are performed twice: with and without fresh air supply and for the following cases:

- step in the emitter power (100% - 0% - 100%) of the radiator
- step in the heat exchange at the external wall by changing the surface temperature (100% - 0% - 100%)
- step in the power of the load simulators (100% - 0% - 100%)

The closed loop tests contain three periods. From one period to another, the heat emitted by the load simulators is changed in order to produce a perturbation in the zone and a reaction of the controller. The values of the gains vary from 30% to 70% of the nominal power of the radiator depending on the period.

## STUDY OF MEASURED SENSOR AIR AND CENTRE AIR TEMPERATURE

In a first step, the air temperatures at different positions in the zone are studied. The measured air temperature at the centre of the zone is compared with the air temperatures measured at two different sensor positions. These positions are near the wall opposite the emitter and near the wall next to the emitter. The measurement sensors are positioned at a height of 1.5m and a distance of 5cm from the walls.

A time delay as well as a slower time response is observed comparing the centre air temperature and the sensor temperatures (figure 5). The temperature response at the two sensor positions is nearly identical. The wall jets at the wall near and opposite the radiator thus seem to be similar.

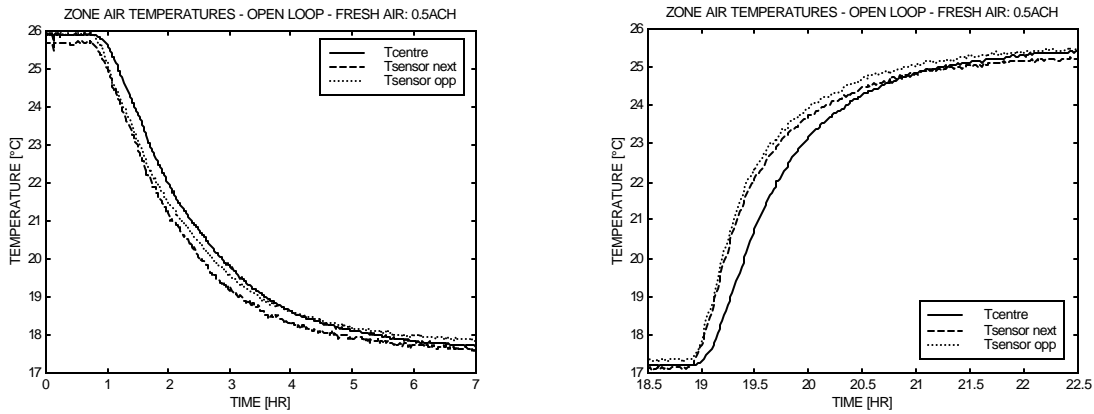


Figure 5: Temperature response at the centre and at two sensor positions (open loop test) for a step from 100% to 0% and vice versa

For the step from 100% to 0% a time delay is observed followed by a similar response time of the temperature. This is due to the position of the sensor in the area of the wall jet. A reduced heat power of the radiator is first measured in the wall jets and then at the centre of the zone.

In the second case, the step of the radiator from 0% to 100%, a time delay as well as a difference in time response between the centre air temperature and that at sensor position is observed. The response time at the sensor position is about 30 minutes while the response time at the centre is about 45 minutes. This results in a temperature difference of up to 2K between centre air and sensor air temperature. The mean temperature values in static conditions are nearly identical.

In the closed loop tests, the effects of these phenomena are analysed for higher frequencies. The test is carried out for a controller with good control characteristics as well as for a controller with bad characteristics (ON/OFF controller). In this study, only the bad controller case is treated. The set point is at 25°C and the valve is equipped with a drive taking about 3-4 minutes to change from the opened position to the closed one.

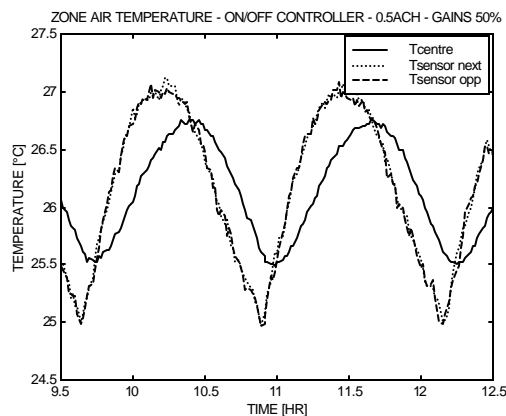


Figure 6: Response of the air temperature at the centre and at two sensor positions (closed loop test) for 50% internal gains

As already observed in the open loop tests, the temperatures at the sensor positions (near and opposite the radiator) are nearly identical, they don't need to be distinguished in the model. Figure 6 presents the result for the second period (50% internal gains).

The temperature at the sensor position reacts quicker than the air at the centre. The response is quicker for the radiator in both ON/OFF periods. The difference in response time between the centre air temperature and sensor air temperature in the three periods can be over 100% depending on the period (internal gains). The difference of centre and sensor air temperature in their amplitude varies from 30% (70% gains) to 100% (30% gains). A phase lag of 10° (70% gains) to 35° (30% gains) for the minima of the oscillation is observed. For the maxima of the oscillation, the corresponding values

vary from 35° (30% gains) to 57° (50% gains). Table 2 shows the obtained values for the second period.

Table 2: Analysis of the results of closed loop test (ON/OFF controller)

Period 2 (50% gains)	$\vartheta_{\text{centre}}$	$\vartheta_{\text{sensor}}$
Mean value [°C]	26.2	26.0
Amplitude [K]	1.2	2
Phase delay of min [°]	Ref.	28
Phase delay of max [°]	Ref.	57

The results of both tests show differences in the following criteria:

- Time delay between centre air temperature and sensor air temperature
- Response time of centre air and sensor temperature
- Phase lag between the temperatures (closed loop tests)

These differences depend mainly of the load of the radiator. It is thus difficult to solve this problem by adding a simple time delay between the sensor- and the centre air temperature ([Klin99]). This solution requires experimental results and is not valid for different frequency domains.

In the following the criteria for a zone model, adapted to control applications, are defined.

### ZONE MODELS FOR CONTROL STUDIES

An adapted model for control studies in the case of the coupling of a zone and an emitter should have a complexity as low as possible. The model must be valid for other room sizes and room types. The important phenomena for the application shall be included in the model. The adapted complexity level of any model for control studies in general is shown in figure 7.

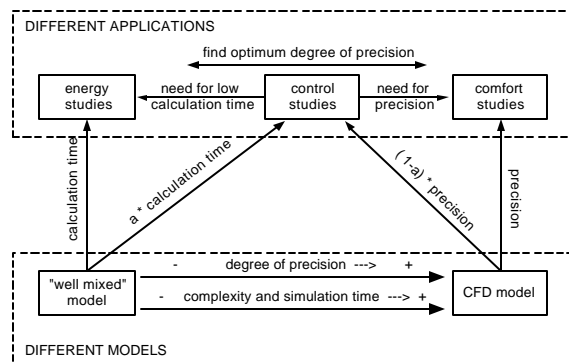


Figure 7: Complexity level of models adapted to a specific application

The needed degree of precision (horizontal position in figure 14) is characteristic for the specific coupling of a zone and an emitter (e.g. with a radiator or a chilled ceiling).

The aim is thus to find the important criteria for a specific coupling of an emitter and a zone.

These criteria for the development of a zone model can be divided in three main parts:

- general characteristics
- parameterisation and validity
- outputs

A chart including these criteria can be constructed in order to obtain a concrete list of characteristics of such a model (table 3). Each model type mentioned in the chart is classed by a fuzzy classification. Six models are compared in the chart:

- second order model (resultant- and wall temperature)
- third order model (with constant coefficients)
- third order model (with variable coefficients)
- Simple zonal model (no pressure calculation)
- Detailed zonal model (higher number of zones, pressure calculation)
- CFD model

However, no existing model have been used to calculate the temperature at the sensor position in transient conditions. Most models use an approach assuming the temperature in the wall jet between the air temperature at the centre and the surface temperature. This is, as showed in the experimental study (cf. precedent chapter), not correct for the transient case.

The division of zonal models in two parts, simple and detailed considers the different types of zonal models. New models have been developed with a higher number of zones. The inter-zonal air flow rates are calculated from the pressure difference between both zones ([Bou93],[Wur95]). The simple zonal models correspond to the type of model developed by Laret [Lar80], During [Dur94], Horwarth [Hor83] or Ngendakumana [Nge88]. They only use correlation or experimental data in their models.

The simple zonal model will be chosen for further development. The simulation time is not increased by the pressure calculation that is necessary for the detailed zonal model. The risk of non-convergence is also lower for this type of model. The available data from this model is enough for control studies. Any further data would increase the complexity of the model without relevant advantages. The model includes the main phenomena at the sensor positions. The necessary number of zones for the different will be defined in a future study. Also, a general representation will be developed in order to enable a simple implementation of the different models in the graphical interface.

In the following, two third order models (cf. table 3) are tested for a control application of a zone equipped with a radiator. The difficulties shall be demonstrated in this application in order to get a concrete list of rules for the development of the zonal model.

Table 3: Criteria for the development of the zone model (fuzzy classification: ++ best; -- worst; n.a. not available)

	Criteria of model	2 <sup>nd</sup> order	3 <sup>rd</sup> order (cst. coeff.)	3 <sup>rd</sup> order (var. coeff.)	Simple zonal model	Detailed zonal model	CFD model
General characteristics	Possibility of real time simulation	YES	YES	YES	YES	YES	?
	Calculation time	++	++	+	o	-	--
Parameterisation and validity	Easy parametering	++	+	+	o	o	--
	Complexity and coherence of initial and boundary conditions	++	++	++	+	+	--
	Validity for different zone type (heavy/light)	+	+	+	Depends on wall modelling		
	Validity for different geometry	+	+	+	+	+	-
	Validity for different zone use	+	+	+	+	+	-
Model outputs	Centre air temperature	n.a.	o	o	+	+/++	++
	Mean radiant temperature	o	o	o	Depends on wall modelling		
	Resultant temperature	o	o	o	Depends on wall modelling		
	Inhomogeneity of horiz. temperature	n.a.	n.a.	n.a.	o	+	++
	Inhomogeneity of vertical temperature	n.a.	n.a.	n.a.	+	+	++
	Mean air velocity	n.a.	n.a.	n.a.	n.a.	o	++
	Temperatures at sensor positions	n.a.	n.a.	n.a.	o	+	++
	Air velocity at sensor position	n.a.	n.a.	n.a.	o	+	++

## VALIDATION OF EXISTING ZONE MODELS

The validation is carried out with a coupled model of a radiator and an existing zone model. The implementation of the models in the graphical environment ([SIM98]) is carried out using a methodology for graphical programming ([Hus99]). The radiator model has been validated in a previous study in static and in transient conditions and also for lower flow rates ([Rie99]).

This coupled model is used for the validation of the zone model by comparison with experimental data for three different cases:

- Simulation of open loop tests (1): the inputs for the coupled model are taken from the open loop tests (c.f. figure 8a);
- Simulation of closed loop test (2): all inputs for the coupled model are provided by the measurements. The controller is not simulated in this case (c.f. figure 8a);

- Emulation of closed loop test (3): The real controller provides the necessary data for the coupled model (c.f. figure 8b)

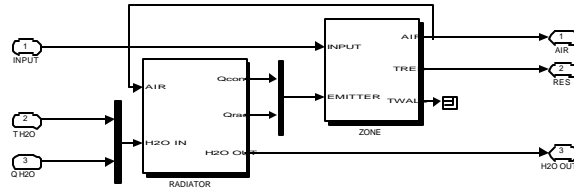


Figure 8a: Coupling of zone model and radiator model for simulated cases (1) and (2)

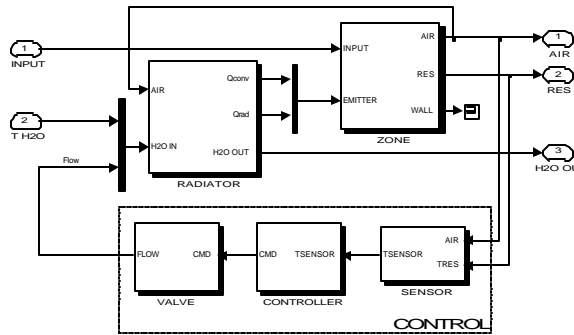


Figure 8b: Coupling of zone model and radiator model for the emulated case (3)

The next chapter describes the validation of an existing zone model of third order. The model is modified for a better fit with experimental data. The validation results are shown for both models for the three cases.

### DESCRIPTION OF THE EXISTING THIRD ORDER MODEL (R5C3)

The existing zone model is a third order state space model with the three states: the air temperature  $\vartheta_i$ , the resultant temperature  $\vartheta_s$  and the wall temperature  $\vartheta_w$ . The model is based on the electric – thermal analogy and has five resistances and three capacitors. A similar model has been developed within a European project for the study of summer comfort in buildings [Mil97]. The electrical circuit of the model is shown in figure 9.

The model includes three resistances connecting “external” temperatures to the three internal temperature nodes.

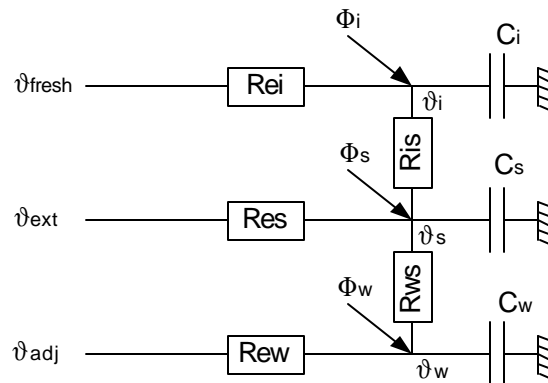


Figure 9: Electrical circuit of the third order model (R5C3)

The first resistance  $R_{ei}$  represents the inverse of the capacitive flow rate of air into the zone: the fresh air supply. The second one,  $R_{es}$ , represents the thermal resistance of the light wall structure between external conditions and the resultant temperature. The third one,  $R_{ew}$ , represents the thermal resistance

between “external” condition and the wall node. Two other resistances connect the wall temperature with the resultant temperature and the resultant with the air temperature.

In the case of the test cell, the external temperatures are as follows:

- Temperature of fresh air supply  $\vartheta_{\text{fresh}}$
- Temperature of the insulated metal panels  $\vartheta_{\text{adj}}$
- Temperature of the non-isolated metal panel (window simulator)  $\vartheta_{\text{ext}}$

The three capacitors are the thermal capacity of the room air, the capacity of the light wall structure (in this case only the thermal mass of the gain simulators) and the capacity of the walls (polystyrene). The heat, injected to the zone by radiation and by convection, is divided into three parts: the convective part to the air node, the radiative part to the two nodes of the wall structure. The equations for the three nodes are as follows:

$$\frac{d\mathbf{J}}{dt} = \left[ \frac{1}{C_i} \left( -\frac{1}{R_{is}} - \frac{1}{R_{ei}} \right) \mathbf{J}_i + \frac{1}{C_i R_{is}} \mathbf{J}_s \right] + \left[ \frac{1}{C_i R_{ei}} \mathbf{J}_{\text{fresh}} + \frac{1}{C_i} \Phi_i \right] \quad (1)$$

$$\frac{d\mathbf{J}_s}{dt} = \left[ \frac{1}{C_s R_{is}} \mathbf{J}_i + \frac{1}{C_s} \left( -\frac{1}{R_{is}} - \frac{1}{R_{ws}} - \frac{1}{R_{es}} \right) \mathbf{J}_s + \frac{1}{C_s R_{ws}} \mathbf{J}_w \right] + \left[ \frac{1}{C_s R_{es}} \mathbf{J}_{\text{ext}} + \frac{1}{C_s} \Phi_s \right] \quad (2)$$

$$\frac{d\mathbf{J}_w}{dt} = \left[ \frac{1}{C_w R_{ws}} \mathbf{J}_s + \frac{1}{C_w} \left( -\frac{1}{R_{ws}} - \frac{1}{R_{ew}} \right) \mathbf{J}_w \right] + \left[ \frac{1}{C_w R_{ew}} \mathbf{J}_{\text{adj}} + \frac{1}{C_w} \Phi_w \right] \quad (3)$$

The convective and radiative heat emission of the emitter and the internal gains is divided into three parts:

- the convective emission is injected to the air node:

$$\Phi_i = \mathbf{e}_{em} \Phi_{em} + \mathbf{e}_{\text{gain}} \Phi_{\text{gain}} \quad (4)$$

- the radiative emission is divided in two parts. One part is injected to the node of the resultant node ( $\Phi_s$ ), one to the wall node ( $\Phi_w$ ):

$$\Phi_s = \mathbf{a}_s \left[ (1 - \mathbf{e}_{em}) \Phi_{em} + (1 - \mathbf{e}_{\text{gain}}) \Phi_{\text{gain}} \right] \quad (5)$$

$$\Phi_w = \mathbf{a}_w \left[ (1 - \mathbf{e}_{em}) \Phi_{em} + (1 - \mathbf{e}_{\text{gain}}) \Phi_{\text{gain}} \right] \quad (6)$$

The calculation of the two factors  $\alpha_s$  and  $\alpha_w$  as well as the calculation of the resistances is shown in the appendix.

The implementation in the used graphical interface is carried out using the general state space representation:

$$\dot{X} = AX + BU \quad (7)$$

$$Y = CX \quad (8)$$

with the following vectors:

$$\begin{aligned} X &= [\mathbf{J}_i, \mathbf{J}_s, \mathbf{J}_w]^T \\ U &= [\mathbf{J}_{\text{fresh}}, \mathbf{J}_{\text{ext}}, \mathbf{J}_{\text{adj}}, \Phi_{em}, \Phi_{\text{gain}}]^T \\ Y &= X \end{aligned}$$

The matrices A, B and C are obtained directly from equation (1) to (8).

## EXPERIMENTAL COMPARISON OF THE THIRD ORDER MODEL FOR THE OPEN LOOP CASE

The model is first compared to the results of the open loop tests. The simulated temperature is in good agreement with the measurements when the radiator is on. If the radiator is not heated, the simulation results are lower than the experimental values.

This difference is due to a lower heat transfer coefficient at the inner room surfaces. An improved model is developed in order to correct this error since the radiator in part load regime appears often in control studies. The results of the experimental validation are presented together with the results of the improved model.

### DESCRIPTION OF AN IMPROVED THIRD ORDER MODEL (R7C3)

In this second model, a fourth temperature  $\vartheta_p$  is added in the electrical scheme. The temperature represents the mean air temperature in the radiator plume. This separate calculation of the temperature in the radiator plume takes automatically into account the variable heat transfer between the cold window and the radiator plume (function of temperature difference). Also a variable heat transfer coefficient by convection between the radiator plume and the external wall can be integrated. This improves the simulation results for transient cases where the heat, emitted by the radiator, changes. The electrical circuit of the modified model is shown in figure 10:

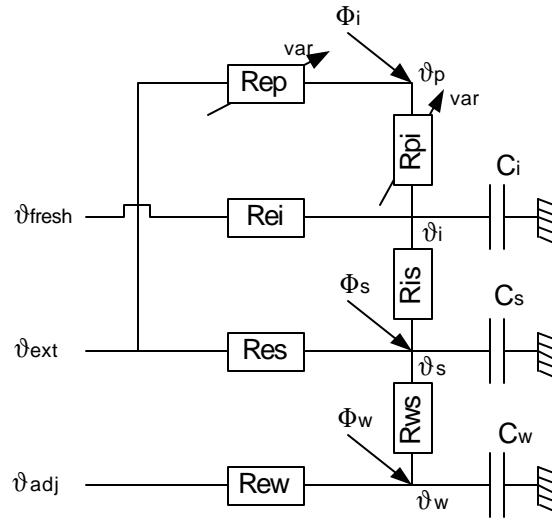


Figure 10: Electrical circuit of the improved zone model (R7C3)

The modification requires a characterisation of the airflow in the radiator plume. Therefore, a correlation is used to calculate the airflow rate as a function of the emitted heat by convection ([Ina88]):

$$\dot{m}_p(z) = 9.51 \cdot 10^{-3} \cdot e_{em} \Phi_{em}(z)^{1/3} (z - z_0) \quad (9)$$

The correlation is used to calculate the airflow at the height of the ceiling ( $z=H_{ceil}$ ). This airflow is entering the radiator plume throughout the height of the zone and is leaving the plume at the ceiling. The variable convective heat exchange coefficient varies depending on the convective heat emitted by the radiator [Dur94]. The state space representation for the nodes  $T_s$  and  $T_w$  in this model is identical to that in the standard model. Equation (1) and (2) are thus the same as for the first model. The equation for the air node (temperature  $T_i$ ) is changed to:

$$\frac{d\mathbf{J}_i}{dt} = \left[ \frac{1}{C_i} \left( -\frac{1}{R_{is}} - \frac{1}{R_{ei}} - \frac{1}{R_{pi}} \right) \mathbf{J}_i + \frac{1}{C_i R_{is}} \mathbf{J}_s \right] + \left[ \frac{1}{C_i R_{pi}} \mathbf{J}_p + \frac{1}{C_i R_{ei}} \mathbf{J}_{fresh} \right] \quad (10)$$

A supplementary static equation is added to calculate the mean temperature in the radiator plume:

$$\frac{(\mathbf{J}_i - \mathbf{J}_p)}{R_{pi}} + \frac{(\mathbf{J}_{ext} - \mathbf{J}_p)}{R_{ep}} + \Phi_i = 0 \quad (11)$$

With equation (11)  $\vartheta_p$  can be eliminated in equation (10) and one obtains the same state space structure as before (equations (7) and (8)), but with different matrices.

$$\frac{d\mathbf{J}_i}{dt} = \left[ \frac{1}{C_i} \left( -\frac{1}{R_{is}} - \frac{1}{R_{ei}} - \frac{1}{R_{pi}} + \frac{1}{1 + \frac{R_{pi}}{R_{ep}}} \right) \mathbf{J}_i + \frac{1}{C_i R_{is}} \mathbf{J}_S \right] + \left[ \frac{1}{C_i R_{ei}} \mathbf{J}_{fresh} + \frac{1}{C_i \left( 1 + \frac{R_{ep}}{R_{pi}} \right)} \mathbf{J}_{ext} + \frac{1}{C_i \left( \frac{1}{R_{pi}} + \frac{1}{R_{ep}} \right)} \Phi_i \right] \quad (12)$$

The matrices A and B, constant for the simple model, are both variable during the simulation depending on the controlled input U(4), the emission of the radiator  $\Phi_{em}$ .

$$\dot{X} = A(\Phi_{em}) X + B(\Phi_{em}) U \quad (13)$$

## COMPARISON OF THE OPEN LOOP CASE AND THE SIMULATED CLOSED LOOP CASE

The simulation as well as the emulation results can be improved by using the R7C3 model. The first step, as mentioned before, is the introduction of a variable convective heat transfer coefficient between the radiator plume and the window. Figure 11 compares the results obtained with both models in an open loop test with a step in the emitter power.

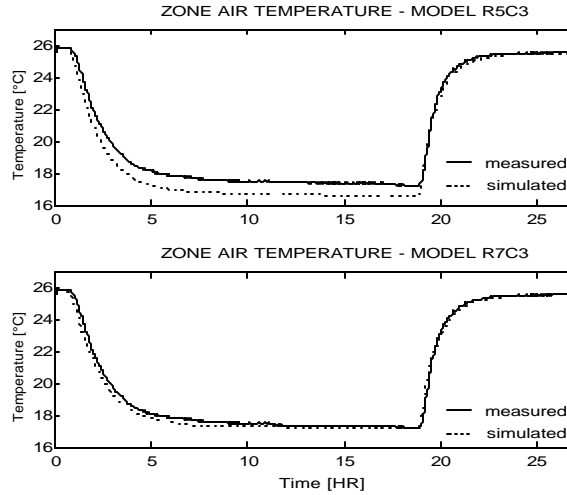


Figure 11: Zone air temperature from the two models for a step in the radiator power

The R7C3 model gives a better representation of the non-heated cell and keeps the same accuracy as the R5C3 model when the radiator is on. The simulated behaviour of the closed loop test thus will be more promising with the R7C3 model as the load of the radiator changes continuously.

For all other open loop tests both models give similar results; the improved model can thus be applied in any case.

Both models are now compared in a simulation of the test with controller. The water flow rate in the radiator is taken from experimental data. With this simulation, the models shall be tested for higher frequencies and shall be adjusted, if necessary, for the emulation of the whole closed loop test. Both models output a too low air temperature in all three periods of the test (figure 12). For both models the accuracy is better in the third period, where the mean power of the radiator is the highest. The heat exchange coefficient is, in this third period, closer to that validated in the open loop tests. In general, the R7C3 model gives closer results to the experimental data as the R5C3 model. The correction of the injected convective heat by the supplementary air node is relevant. The validation shows that the

standard model give satisfying results for all cases that are close to the nominal power of the radiator. As the radiator works in part load regime, the accuracy of the R5C3 model decreases. Figure 12 shows this phenomenon in the first and the second period.

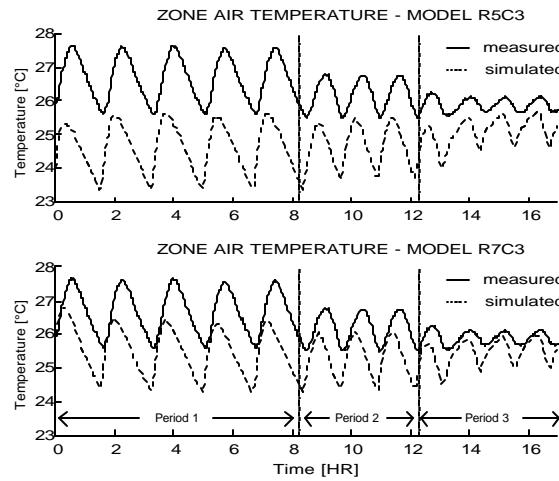


Figure 12: Zone air temperature from the two models for the simulation of the controller test

### ADJUSTMENT OF THE ZONE MODELS

The R7C3 model corrects this error partially. The accuracy is better in all three periods. However, an error remains depending on the load. The lower the mean power of the radiator is, the higher the error is. This phenomenon has not been observed in the open-loop tests since the temperature in the zone was about 17°C. The convective heat exchange at the external wall thus was lower than in the closed loop test. In the tests with controller, the air temperature is always about 25°C, the convective heat exchange at the external wall is higher. The higher temperature difference between the zone and the external wall makes the heat transfer by convection more sensible for a change in the radiator power. This problem is more visible in the case of the test cell than in a normal room. The use of a “window simulator”, the cooled wall, that has a constant temperature, does not correspond to a case observed in a normal room. When the emitter works in part load conditions, the temperature of this wall or window is also changing. In the case of the test cell, the temperature of the window is fixed. The heat losses through the window thus are much higher than in reality. The effect of a change of the heat exchange coefficient by convection is so more important (cf. equation (24) in the appendix). However, the problem has to be solved in order to get a good agreement in the emulation of the controller test. Obviously, the general heat exchange coefficient by convection is lower in the closed loop tests than in the open loop tests. This coefficient is reduced to fit with experimental data in order. The new value is 30% lower as the coefficient used during the open loop tests. This enables a correct emulation. The effect of the changing heat transfer coefficient can also be seen in the heat balance of the radiator. The emitted power in this case would be much higher than in reality. The result of the reduction of the general heat transfer coefficient by convection is shown in figure 13.

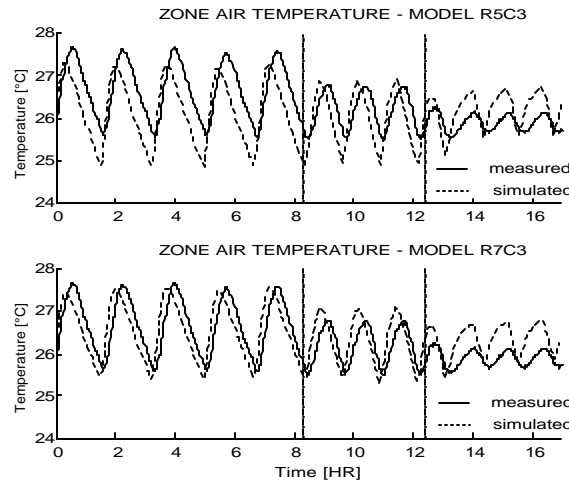


Figure 13: Zone air temperature for the simulation of the controller test with adjusted convective heat transfer coefficient

For the standard model, temperature amplitude as well as mean value differ slightly in all three periods. The improved model gives better results in the first and the second period. The third period differs in a similar way as in the standard model. It is important to guarantee a good agreement in the period with the highest radiator load (period 3) for the emulation. If the convective heat exchange coefficient would be too high in this period (and thus the heat losses too high), the system could be out of control because of a too low emission of the radiator. In the following chapter, the models are validated by emulation using the adjusted parameters of the model.

#### VALIDATION OF THE R7C3 MODEL BY EMULATION

The emulation of the measured cases includes separate dynamic models representing the controller sensor, the valve and the drive (cf. figure 7). The controller used in this emulation is a simple ON/OFF controller.

Particular attention is paid to the model of the controller sensor. The emulation results are very sensible to this model. A wrong estimate of the temperature measured by the sensor results in a wrong mean temperature value in the zone. This changes the load of the radiator and thus the temperature control, too.

The sensor is modelled as a first order. As the manufacturer of this controller was not involved in this study, the percentage of the air/radiant temperature and the time response of the sensor were unknown to the authors. Measurements are thus carried out in order to define these values. However, it is difficult to determine the percentage of air and radiant temperature. Small changes of these values are carried out in pre-emulations in order to adjust the mean values as well as the periods of the control oscillations. The heat balance on the radiator confirms the correct values of the parameters of the sensor model. The behaviour of the air temperature near the controller sensor (input to the sensor model) can be taken into account in the following ways:

- Adjustment of the model of zone (sensor temperature is modelled instead of mean air temperature  $\vartheta_i$ ;
- A time delay is added between the sensor air temperature and the centre air temperature ([Klin99]);
- The sensor model is adjusted in order to keep the parameters of the zone model.

In this study, the third possibility is chosen, since, in any case, the controller sensor brings the highest uncertainties.

The used value for the time constant is 1200s. The percentage of air/radiant temperature is set to 20/80. This value is reasonable since the sensor box is closed; no air can enter into the sensor box. The results are shown in figure 14. The air temperature and the resultant temperature are compared.

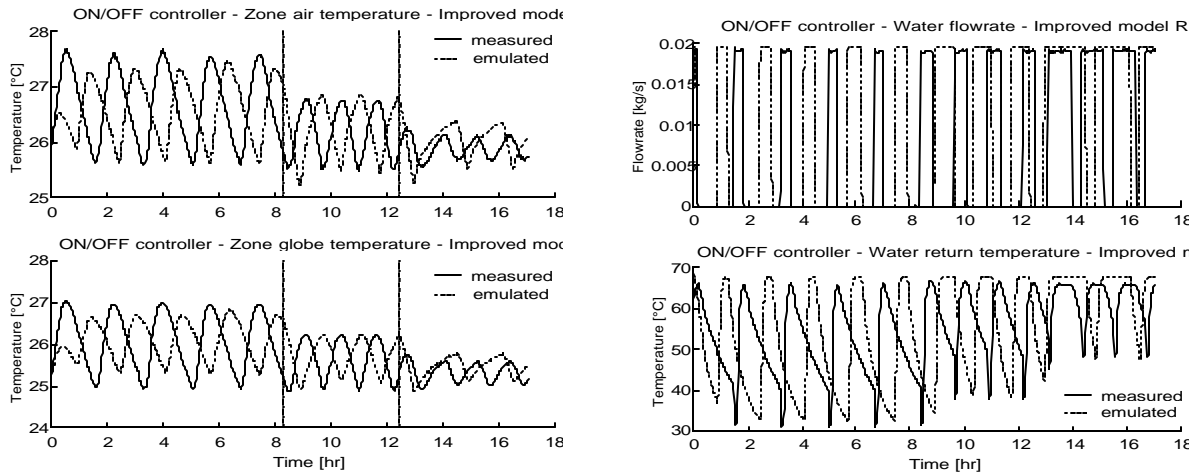


Figure 14: Emulation results for the improved model R7C3

The results obtained in the first and in the second period show good agreement with the experimental data except for a time shift. The time shift is due to the initialisation of the models and the initial position of the valve.

In the third period, the air temperature differs from the measured value. The mean value corresponds to the measurements, while the amplitude and the period of the air temperature differ. The water flow rate in the radiator, obtained in the emulation, shows this difference, too. The periods with mass flow are about 50% longer than in the measured case. The reasons for this discrepancy have not been found yet.

### COMMENTS ON THE RESULTS

The results obtained are close to the measurement. A classification of the controller ([TC247]) would have been nearly identical for the measured case as well as for the emulated case. However, the adjustment undertaken in the preparation of the emulation limits the applicability of the model. If the zone size is changed, the model is not valid. The following comments shall explain the problems that appeared during the modelling and the emulation:

- the standard model gives acceptable results in the emulation if the emitter load is near the nominal power
- the improved model produces more acceptable results for all emitter loads after adjusting the parameters of the zone model and the sensor model

The open loop tests do not need an adjustment of the parameters. The models agree well with the measurements. In the controller test, some parameters of the zone model and the sensor model have to be adjusted. These parameters are:

- convective heat transfer coefficient of zone model
- response time of the sensor model
- partition of air/radiant temperature in the sensor model

The introduction of a supplementary air node representing the radiator plume as well as the variable heat transfer coefficient by convection improved the results. The values for this coefficient for all other surfaces are modelled constant. A more detailed model with variable values for the ceiling could improve the results. The results in all three periods should be improved with this type of model.

The adjustment of the parameters of the sensor model hide the differences between simulated centre air temperature and the real air temperature at the sensor position. The result of the emulation is very sensible to these parameters. A zonal model, taking into account this difference, could solve this problem. Such a type of model would reduce the adjustment of parameters. It would represent a model with better accuracy and would be valid even for different room sizes or types. Also, the sensor could be modelled more detailed since the necessary inputs are available from a zonal model.

### CONCLUSION

The difference between the temperature at the position of a controller sensor and the centre air temperature is analysed by experiment in this study. Both air temperatures can differ in their static as well as in their transient conditions. This difference can be important for the study and the development of room controllers depending on the convective phenomena in the zone.

For the development of controllers it is of major importance to know where the sensor of a controller is placed since the sensor position affects the result of the control. If a control algorithm or a real controller shall be tested by simulation or by emulation, it is necessary to model correctly all important phenomena.

In this study two simplified third order models are applied to an emulation of a controller evaluation in order to test the results and the applicability of simplified models (usually used for control studies). Correct results can be obtained using these simple models by slightly adjusting the parameters to the results obtained by experiment. The possibilities are explained in the study. However, the result rests uncertain for non-validated cases since the adjustment of parameters is only valid for a single case.

The experimental comparison of sensor- and centre air temperature as well as the result from the simplified models encourage the development of a zonal model taking into account the important phenomena (listed in this paper). Such a model would be valid for different cases without an adjustment of parameters.

In a next step, this kind of model will be developed. A general representation in a graphical programming environment will be developed in order to permit an application for different emitter types. This more detailed modelling approach enables also a more detailed modelling of the controller sensor.

The resulting models will be more adapted for the development and the test of controllers. The simplicity concerning their parametering and their use makes them interesting for manufacturers of controllers as well as for research laboratories carrying out studies in the control field.

## ACKNOWLEDGEMENTS

All experimental tests have been carried out at WSP-Lab, Stuttgart, Germany.

## NOMENCLATURE

### English letter symbols:

$\dot{m}$	Flow rate	[kg/s]
A	surface	[m <sup>2</sup> ]
C	Thermal capacity	[J/K]
$c_p$	Thermal heat capacity of air	[J/(kg*K)]
Q	Flow rate	[kg/s]
R	Resistance	[K/W]
T	Temperature	[K]
U	U-value for wall or window	[W/K]
U	Input vector	[-]
V	Volume	[m <sup>3</sup> ]
X	State vector	[-]
Y	Output vector	[-]
z	Height	[m]

### Greek letter symbols:

$\alpha$	Percentage distributing radiative heat	[-]
$\delta$	Thickness of wall layer	[m]
$\varepsilon$	Partition of convective heat flux of emitter	[-]
$\Phi$	Heat flux	[W]
$\vartheta$	Temperature	[°C]

### Subscripts:

cond	conductive
conv	convective
em	emitter
ext	external
fresh	fresh air supply
gain	internal heat gain
heavy	heavy wall structure
i	Air

light	light wall structure
p	plume
rad	radiative
s	Resultant
tot, t	total
w	Wall
win	window

## BIBLIOGRAPHY

- [Bou93] Bouia, Modélisation simplifiée d'écoulements de convection mixte interne: Application aux échanges thermo-aérauliques dans les locaux, PhD Thesis, University of Poitiers, 1993
- [DOE2] Overview of the DOE-2 program, Version 2.1D. Simulation Research Group, Lawrence Berkeley Laboratory, LBL-19735, 1989
- [Dur94] During, Consommations énergétiques et confort thermique des locaux chauffés: approche par les modèles zonaux, PhD thesis, INSA Lyon, 1994
- [Hav98] Haves, A standard simulation test bed for the evaluation of control algorithms and strategies, ASHRAE Transactions, 1998, Vol. 104, Part 1
- [Hor83] Horwarth, Temperature distributions and air movements in rooms with a convective heat source, PhD thesis, University of Manchester, 1983
- [Hus97] Husaunndee, SIMBAD : A simulation toolbox for the design and test of HVAC control systems. Proceedings of the 5<sup>th</sup> international IBPSA conference, Prague, CZECH REPUBLIC, 2 : 269-276
- [Hus99] Husaunndee, The building HVAC System in control engineering- A modelling approach in a widespread graphical environment, ASHRAE transactions , 1999, Vol. 105, Part 1
- [Ina88] Inard, Contribution à l'étude du couplage thermique entre un émetteur de chaleur et un local, PhD thesis, INSA Lyon, 1988
- [Kast98] Kast, Dynamischer Anlagensimulator für Heiz- und RLT-Anlagen, Gesundheitsingenieur, 119, 1998
- [Klin99] Klinger, Bedarfsgerechte Regelung des Raumluftzustandes in Wohngebäuden – Teil 1-2, HLH, Bd. 50, 1999
- [Lar80] Laret, Contribution au développement de modèles mathématiques du comportement thermique transitoire de structures d'habitation, PhD thesis, University of Liège, 1980
- [Mil96] Millet, Confort d'été dans l'habitat – Méthode de calcul de référence: hypothèses et algorithmes, V1.3, ENEA/CVA-97.083Rd, 1997
- [Nge88] Ngendakumana, Modélisation simplifiée du comportement thermique d'un bâtiment et vérification expérimentale, PhD thesis, University of Liège, 1988
- [Os96] Osman, Model- based control of laboratory HVAC systems, PhD thesis, University of Wisconsin, 1996
- [Peng96] Peng, Modelling of indoor thermal conditions for comfort control in buildings, PhD thesis, Delft, University of Technology, 1996
- [PHO91] PHOENICS, Reference manuals, CHAM Company, UK 1991
- [Rat98] Ratnam, Advanced feedback control of indoor air quality using real-time computational fluid dynamics, ASHRAE transactions, 1998, Vol. 104, Part 1
- [Rie99] Riederer, Analyse du modèle de radiateur, rapport interne CSTB, unpublished, 1999
- [Rou97] Rouvel, Ein regelungstechnisches Modell zur Beschreibung des thermisch dynamischen Raumverhaltens, Teil 1-3, HLH, Bd. 48, 1997
- [Sim98] SIMULINK dynamic System Simulation for Matlab. Version 2.1 Mathworks Inc., Ma., USA, 1998
- [TC247] European standard, Controls for mechanical building services, 1999
- [TRN96] TRNSYS, A transient Simulation Program. Solar Energy laboratory of the University of Wisconsin; Madison, USA, 1996
- [Wur95] Wurtz, Modélisation tridimensionnelle des transferts thermiques et aérauliques dans le bâtiment en environnement orienté objet, PhD thesis, Ecole Nationale des Ponts et Chaussées, Paris, 1995

## APPENDIX

### Definition of the resistances in the R5C3 model

- $R_{ei}$  : thermal resistance representing the fresh air supply to the zone

$$R_{es} = \frac{1}{\dot{m}_{fresh} c_p} \quad (14)$$

- $R_{es}$  : thermal resistance representing the rapid heat exchange between the internal and external conditions via the lightweight building structure

$$R_{es} = \frac{1}{U_{light}} \quad (15)$$

- $R_{is}$  : thermal resistance between the air node and the resultant node

$$R_{is} = \frac{\frac{1}{h_{conv}} - \frac{1}{h_{tot}}}{A_t} \quad (16)$$

- $R_{ws}$  : thermal resistance between the resultant temperature and the internal surface of the heavy wall structure

$$R_{ws} = \frac{1}{h_{tot} A_w} \quad (17)$$

- $R_{ew}$  : thermal resistance between the external conditions and the internal surface of the heavy wall structure

$$R_{ew} = \frac{1}{U_{heavy}} - R_{ws} \quad (18)$$

- $C_i$  : Thermal capacity representing the internal room air

$$C_i = \mathbf{r}_i c_{p_i} V_i \quad (19)$$

- $C_s$  : Thermal capacity representing the lightweight structure

$$C_s = \sum_i C(i) \quad (20)$$

$$C(i) = \sum_k \mathbf{r}(k) \mathbf{d}(k) A(k) c_p(k)$$

Subscript i refer to the lightweight structure layers. Subscript k refer to the different wall layers.

- $C_m$  : Thermal capacity of the heavy-weight structure

$$C_w = \sum_p A(p) ac(p) \quad (21)$$

$$A_w = \frac{C_w^2}{\sum_p A(p) ac(p)^2}$$

Subscript p corresponds to the heavy-weight structure. The term  $ac(p)$  is the thermal surface capacity of the heavy wall.

- The radiative heat emission of the emitter and the internal gains are distributed to the wall node and the resultant node using the following expressions:

$$\mathbf{a}_s = \frac{1}{A_t} \left( A_t - A_w \frac{1}{R_{es} h_{tot}} \right) \quad (22)$$

$$\mathbf{a}_w = \frac{A_w}{A_t}$$

- The mean radiant temperature can be calculated by:

$$\mathbf{J}_{mr} = \frac{h_{tot} \mathbf{J}_s + h_{conv} \mathbf{J}_i}{h_{rad}} \quad (23)$$

### Definition of the resistances in the R7C3 model

The calculation of the resistances used in the standard model is identical for this model. There exist two supplementary resistances that have to be defined for the R7C3 model:

- $R_{ep}$  : thermal resistance representing the convective heat exchange between the external conditions and the air in the emitter plume:

$$R_{ep} = \frac{1}{U_{win}} \quad (24)$$

This resistance can be constant or variable. It consists of the heat exchange coefficients by convection, radiation and conduction for the window. In the case of the test cell (internal wall temperature is measured) it consists only of the internal heat exchange by convection. The influence of a small variation of this coefficient is very high for the test cell. In the validations a variable heat exchange coefficient thus is chosen.

- $R_{pi}$  : thermal resistance representing the airflow between the emitter plume and the zone air. The airflow is calculated using a correlation for the mass flow in plumes.

$$R_{pi} = \frac{1}{\dot{m}_{plume} c_p} \quad (25)$$